GEOLOGICA BELGICA (2020) 23/1-2: 87-92

JONGERENDAG - JOURNEE DES JEUNES – 18.10.2019

Abstracts of communications presented at the 'Master Day' meeting, Gent

Holocene vegetation reconstruction of the Zwarte Beek catchment, Campine Area (Belgium). A pollen-based and multivariate statistical approach

FEMKE AUGUSTIJNS[1], LAURA VERVACKE[1], EVELINE SCHERPS[1], RENSKE HOEVERS[1], NILS BROOTHAERTS[1] & GERT VERSTRAETEN[1]

[1]*KU Leuven, Department Earth and Environmental Sciences, Division of Geography and Tourism, Celestijnenlaan 200E, B-3001 Leuven, Belgium.*

Pollen records from all over the globe have proven the dynamic nature of vegetation cover, resulting in dramatic changes in plant community composition and abundances over long time scales, including the current interglacial period. This interval, known as the Holocene epoch, is characterized by an additional factor influencing the established vegetation: apart from climatic and soil conditions, human impact also becomes a significant driver of vegetation changes. In Flanders these Holocene environmental changes are well clarified for the loamy region, but less high-resolution well-dated pollen records are available for the sandy region. Therefore, this study focuses on an over three meter long sediment core from the exceptionally thick peat deposits in the Zwarte Beek valley, situated in the Campine region.

Pollen analysis is chosen as a method to reconstruct the regional vegetation and human impact evolution from the studied peat sequence. In total, 31 levels of peat were studied by extracting and identifying their pollen content. This resulted in a high resolution pollen diagram which was further analysed using multivariate statistics: clustering techniques were used as the basis for the identification of biozones in the vegetation development. Ordination analysis, more specifically NMDS, was applied to detect the major patterns within the pollen data and used as validation of the obtained clusters.

Radiocarbon dating of four levels showed that the peat sequence spanned the interval from ca. 11.4 to 6.7 ka cal BP. A hiatus was detected based on the dating results and the presence of cereals, which indicated a significantly younger age above this level. Several causes were proposed including peat excavation, mineralisation by desiccation and halted peat growth during the Middle Holocene.

Integration of the pollen analysis with plant macrofossils (Vervacke, 2019), macro-charred particles (Scherps, 2019) and climatic data resulted in the subdivision of the Zwarte Beek vegetation development into six biozones (Fig. 1): before 11.2 ka cal BP, an open landscape dominated by grasses, shrubs and pioneer trees was reconstructed. This was followed by the establishment of an open pine woodland with frequent occurrence of fires. From 9.8 ka cal BP temperate trees were introduced in the region and a closed deciduous forest was formed with hazel, oak and elm as the dominant tree types. At 8.5 ka cal BP, a major shift in the local wetland vegetation was observed: where the valley was originally covered with sedges in an open landscape, now a valley forest was formed. This alder carr dominated the local vegetation until 7.8 ka cal BP. From then, the valley was occupied by a mosaic of alder carr, sedges and peat mosses. During this phase the deciduous forest of the regional vegetation became partially opened while heather and grasses expanded. Humans and fire were possibly involved in this vegetation alteration. The Middle Holocene peat sequence continued until 6.7 ka cal BP, after which a hiatus was present until Medieval or recent times. The vegetation composition above this hiatus was strongly opened with abundant grasses and heather. Cereal pollen from buckwheat and rye were identified and peat mosses reached their maximal abundance.

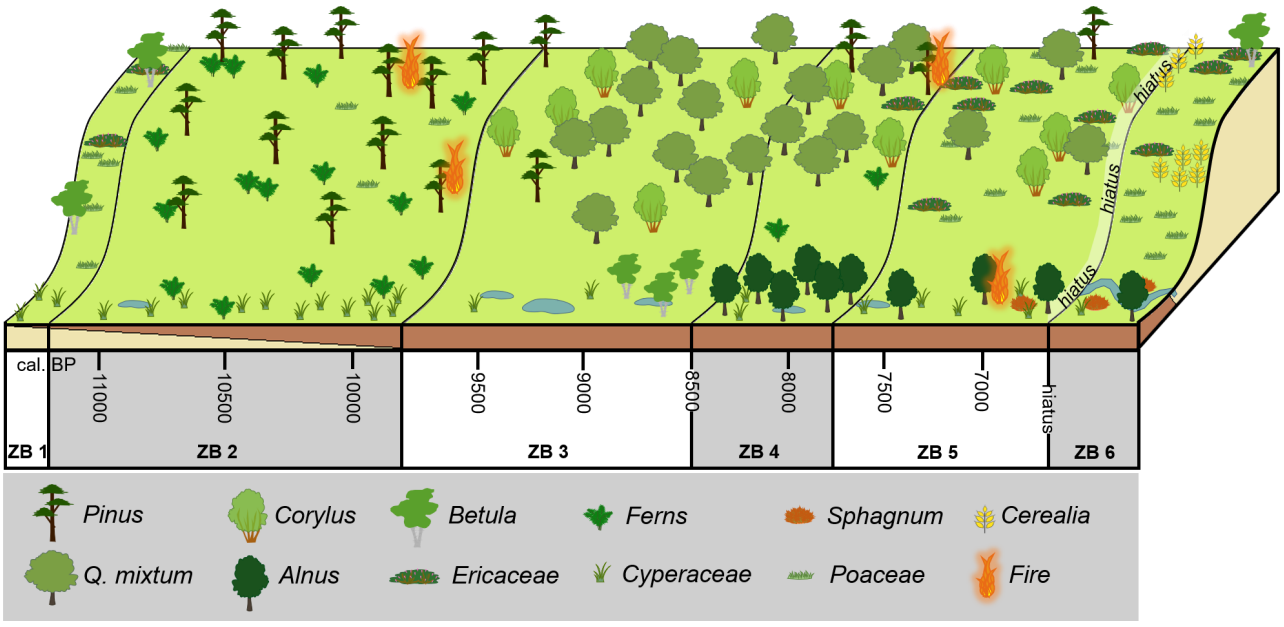

Figure 1. Visualization of the vegetation development in the Zwarte Beek area. The time axis is based on radiocarbon dating of four levels of the peat sequence.

The obtained vegetation evolution for the Zwarte Beek region was compared to previous research on this valley and to adjacent regions within sandy Flanders and the loamy region. This showed that the major Early and Middle Holocene vegetation stages were uniform across Flanders, however the timing of some transitions did differ significantly even over relatively short distances. Finally, a comparison to Eemian pollen diagrams was performed, showing the possibilities and limitations of pollen records as analogues for contemporary vegetation changes.

References

Scherps, E. 2019. Reconstrueren van Holocene Branden in de Vallei van de Zwarte Beek (Vlaanderen). Unpublished Bachelor's thesis, KU Leuven, Leuven.

Vervacke, L. 2019. Reconstructing Holocene changes in floodplain ecology based on plant macrofossils - a case study of the Zwarte Beek Valley, Belgium. Unpublished Master's thesis, KU Leuven, Leuven.

Lake sediment records of late Holocene proglacial floods from the San Lorenzo Icefield (Patagonia)

STIJN ALBERS[1*], ALBERTO ARANEDA[2] & SÉBASTIEN BERTRAND[1]

[1] Renard Centre of Marine Geology, Department of Geology, Ghent University, Krijgslaan 281/S8, 9000 Ghent, Belgium.
[2] Centro de Ciencias Ambientales EULA-Chile, Universidad de Concepción, Casilla 160-C, Concepción, Chile.
[*]corresponding author: Stijn.Albers@UGent.be.

Understanding the past occurrence of river flooding is important to assess future flood risks (Wilhelm et al., 2018) and to understand the impact of climate change on flood occurrence, especially since a warming climate is expected to cause an increase in the frequency and intensity of such events (Seneviratne et al., 2012). Chilean Patagonia, being a glacierized region undergoing climate change, is particularly prone to river flooding triggered by increased rainfall or rapid snow and/or ice melt (e.g. Bertrand et al., 2014; Dussaillant et al., 2010). This study investigates the late Holocene flooding of two proglacial rivers in Chilean Patagonia, i.e. Río Tranquilo and Río del Salto, by using the lake sediments of Laguna Confluencia and Lago Juncal, respectively, as flood archives. Both rivers receive meltwater from glaciers of the San Lorenzo Icefield, which have retreated rapidly over the past century (Falaschi et al., 2013). During floods, the outflows of Laguna Confluencia and Lago Juncal reverse and act as inflows from the proglacial rivers. This occasional flood inflow results in the deposition of distinct flood layers on the lakebed, allowing the reconstruction of flood occurrence through the analysis of short sediment cores.

A multi-proxy data set containing geophysical, geochemical, and sedimentological variables was obtained by performing a series of non-destructive and destructive analyses on five sediment cores. This includes X-Ray Computed Tomography (CT), magnetic susceptibility, gamma-ray density, and X-Ray Fluorescence (XRF) core scanning, and grain size and smear slide analysis. The results of these analyses were used to identify flood deposits and ultimately generate paleoflood records. Furthermore, a sediment accumulation rate based on radionuclide analysis was obtained on the best sediment core to produce a preliminary flood chronology.

When comparing the records of the two studied lakes, flood deposits can more clearly be distinguished from lake background sediment in Laguna Confluencia than in Lago Juncal. This is due to the organic-rich nature of the background sediment in the former lake, allowing the detrital-rich flood deposits found in the lake sediments to stand out. The absence of such organic-rich background sediment in Lago Juncal makes this lake less suitable for paleoflood reconstruction. The clear identification of flood deposits in Laguna Confluencia, however, allows us to reconstruct the flooding history of Río Tranquilo during the last 1200 years. The Laguna Confluencia record contains 54 flood events. Results show the presence of five periods of high flood frequency in 850–1130 CE, 1260–1440 CE, 1570–1620 CE, 1730–1820, and 1920–1970 CE, the most notable of which occurred in 1260–1440 CE. The latter displays 13 floods with an average return period of 9 years.

Comparing the flood history of Río Tranquilo with glacier variability of the San Lorenzo Icefield reveals that river flooding increases after periods of glacier advance, suggesting that the flood events are related to meltwater production. Furthermore, river flooding appears to increase when temperatures are higher. The main cause of river flooding is therefore hypothesized to be an increased snow/ice melt during climate warming. Precipitation does not seem to significantly influence flood occurrence, but it could affect flood frequency during warm periods, such as between 1260 and 1440 CE. Considering the apparent link between flood occurrence and temperature, we hypothesize that flooding of Río Tranquilo will not decrease in the near future. Although core chronology needs to be improved using other dating techniques, for instance, radiocarbon dating, our results support the use of lake sediments as paleoflood archives in the southern Andes. Paleoflood research should therefore be encouraged in Chilean Patagonia to improve the understanding of flood occurrence in the context of glacier and climate variability.

References

Bertrand, S., Hughen, K., Sepúlveda, J. & Pantoja, S., 2014. Late Holocene covariability of the southern westerlies and sea surface temperature in northern Chilean Patagonia. Quaternary Science Reviews, 105, 195–208. https://doi.org/10.1016/j.quascirev.2014.09.021

Dussaillant, A., Benito, G., Buytaert, W., Carling, P., Meier, C. & Espinoza, F., 2010. Repeated glacial-lake outburst floods in Patagonia: an increasing hazard? Natural Hazards, 54, 469–481. https://doi.org/10.1007/s11069-009-9479-8

Falaschi, D., Bravo, C., Masiokas, M., Villalba, R. & Rivera, A., 2013. First Glacier Inventory and Recent Changes in Glacier Area in the Monte San Lorenzo Region (47°S), Southern Patagonian Andes, South America. Arctic, Antarctic, and Alpine Research, 45, 19–28. https://doi.org/10.1657/1938-4246-45.1.19

Seneviratne, S., Nicholls, N., Easterling, D., Goodess, C., Kanae, S., Kossin, J., Luo, Y., Marengo, J., McInnes, K., Rahimi, M., Reichstein, M., Sorteberg, A., Vera, C. & Zhang, X., 2012. Changes in climate extremes and their impacts on the natural physical environment. In Field, C., Barros, V., Stocker, T., Qin, D., Dokken, D., Ebi, K., Mastrandrea, M., Mach, K., Plattner, G., Allen, S., Tignor, M. & Midgley, P. (eds), Managing the Risks of Extreme Events and Disasters to Advance Climate Change Adaptation. A Special Report of Working Groups I and II of the Intergovernmental Panel on Climate Change (IPCC). Cambridge University Press, Cambridge, 109–230.

Wilhelm, B., Ballesteros-Canovas, J., Macdonald, N., Toonen, W., Baker, V., Barriendos, M., Benito, G., Brauer, A., Corella, J., Denniston, R., Glaser, R., Ionita, M., Kahle, M., Liu, T., Luetscher, M., Macklin, M., Mudelsee, M., Munoz, S., Schulte, L. & Wetter, O., 2018. Interpreting historical, botanical, and geological evidence to aid preparations for future floods. WIREs Water, 6, e1318. https://doi.org/10.1002/wat2.1318

Disparity of the mandibles of primitive sabre-toothed felids from the late Miocene of Batallones (Spain)

NARIMANE CHATAR[1*], MANUEL J. SALESA[2], JORGE MORALES[2] & VALENTIN FISCHER[1]

[1]Evolution & Diversity Dynamics Lab, UR Geology, University of Liège, B18, 14 allée du 6 août, 4000 Liège, Belgium.
[2]Departamento de Palaeobiología, Museo Nacional de Ciencias Naturales-CSIC, José Gutiérrez Abascal, 2, 28006 Madrid, Spain.
**corresponding author: narimane.chatar@uliege.be.*

Machairodontinae is a clade of felid carnivorans that has gathered much attention in technical and popular media alike thanks to their particular sabre-toothed morphology. Unfortunately, early taxa are poorly understood because of a patchy fossil record. The late Miocene fossil localities of Batallones (Madrid region, Spain) contain two cavities (Batallones-1 and Batallones-3) with more than 90 percent of carnivoran remains including two early sabre-toothed marchairodontines: *Machairodus aphanistus* and *Promegantereon ogygia*. Even though these two cavities are separated by only about a hundred meters, previous analyses have suggested that the cavities were not contemporaneous due to differences in the faunal assemblages and that a morphological drift could be observed between the different sites, notably for machairodontines. However, these assemblages were never studied in a thorough quantitative framework. We studied 45 mandibles of *Machairodus aphanistus* and *Promegantereon ogygia* as well as 4 mandibles of more derived machairodontines and 8 mandibles of extant felines to test for geographic and temporal differences and to better characterize the morphological position of these important taxa among other felids.

All our analyses (PCA and MANOVA) converge in rejecting the hypothesis of a marked variation of morphology between Batallones-1 and Batallones-3, no matter the method used to reconstruct morphological disparity. The morphospaces derived from 3DGM were also compared to 'traditional' linear morphometry on the same sample and a mantel test confirmed that the position of each individual was not significantly different between the two morphospaces. The positions of *Machairodus aphanistus* and *Promegantereon ogygia* are interestingly closer to extant felines than other sabre-toothed forms and questions the hunting methods of these two early machairodontines. The use of three-dimensional methods also allowed us to reveal that the orientation and large size of the mandibular condyle is a unique feature of machairodontines among Felidae.

Characterisation of the Kačák event (late Eifelian, middle Devonian) and its effects on palaeobiodiversity

VALENTIN JAMART

Evolution & Diversity Dynamics Lab, U.R. Geology, Université de Liège, 14 Allée du Six-Août, B18, Sart Tilman, 4000 Liège, Belgium; valentin.jamart@alumni.uliege.be.

The Devonian is a period that recorded many of bio-crisis. One of them, known as the Kačák event extends along the *Polygnathus ensensis* zone immediately before the Eifelian-Givetian boundary. This crisis was identified in many localities, mostly in bathyal settings. The event, divided into two phases (*otomari* event and Kačák event s.s.), is typically marked by a turnover among pelagic faunas, especially conodonts, dacryoconaridids and ammonoids. This turnover is linked to a transgression associated with anoxia that corresponds in the lithological succession to the deposition of black shale in deep-water settings. In Belgium, the Kačák event s.s. corresponds to a time window equivalent to the deposition of the Lomme and Hanonet formations. Six localities (Baileux, Couvin, Hampteau, Jemelle, Nismes and Resteigne), located on the southern margin of the Dinant Synclinorium exposing the carbonate Hanonet Formation, have been sampled for rugose and tabulate corals. The analysis pinpoints that the Kačák event had a moderate to weak impact on the Belgian carbonate shelf. The Old World Realm faunal assemblages show no significant variation in diversity during the Kačák event. Nevertheless, the remarkable occurrence of rugose corals typical of the East American Realm (siphonophrentids and heliophyllids) in the lower part of the Hanonet Formation helps identify the event as the latter is also marked by a short phase of cosmopolitanism of benthic fauna. This can be used as a marker of the Kačák event especially where the typical pelagic ones are missing.

Fractures roughness analysis in Luxembourg sandstone

SAMIR MOHAMMAD[1], SARA VANDYCKE[2] & MARIE-LAURE WATTIER[2]

[1] *DGES, Université Libre de Bruxelles, Belgium; samir.mohammad@ulb.ac.be.*
[2] *Mining engineering lab, Université de Mons, Belgium; Sara.VANDYCKE@umons.ac.be; Marie-Laure.WATTIER@umons.ac.be.*

Introduction

Fluid flow in fractured rocks is a very important process to study in hydrogeology and engineering and until now all the equations used to estimate flow through fractured rocks are complex and require some simplifications to be used in applications. The most used equation to model fluid flow is the modified Cubic law.

$$Q = \frac{-\nabla p \, w \, e^3}{f \, \mu \, 12} \qquad (1)$$

where Q is the volumic flow rate, ∇p a hydraulic pressure gradient, e is a hydraulic aperture, w is a fracture width, and μ is fluid viscosity.

The cubic law (1) is valid for the main following hypotheses:

- Steady laminar flow, which will be defined by using Reynolds number (Re), which connect inertial forces to viscous forces, (Re) must be less than one (Zimmerman & Bodvarsson, 1996) in order to have a laminar flow;
- Incompressible fluid;
- Single fluid.

The factor (f) is a correction factor related to many parameters including Tortuosity, contact area, channelling and most importantly Roughness which has many definitions but, it is possible to define it as the average asperity heights on the fracture face.

The objective of this work is to analyse fractures roughness in Luxembourg Sandstone (Ernzen quarry) as it considered one of the most important parameters affecting fluid flow in fractured rocks using different methods and define the best-correlated methods.

Methods

Studying the geology and the tectonic context of Trier-Luxembourg Basin (TLB) and construct Rose diagram by defining the direction and dip of 127 joints in order to understand type of deformations and different joint families, then analysing fractures roughness in the field using visual observation (scale 1-3) and using the gauge device to analyse joints roughness profile and compare them to the ten JRC roughness profiles proposed by (Barton & Choubey, 1977).

Studying the mechanical properties of Luxembourg Sandstone, which obtain by performing different tests, including uniaxial compressive test, shear test, Brazilian tensile and triaxial test to understand the behaviour of the rock under compression, tensile and shear stresses, which generate different type of fractures with different surface roughness profiles.

Studying the petrophysical properties of Luxembourg Sandstone (porosity, density and permeability) help to understand the rock properties like pores interconnection, which

control the accumulation and movement of fluids and depend strongly on the roughness of the fractures.

Using a high precision Laser to scan different natural and lab generated surfaces to get raw data and process data by using MATLAB to analyse surfaces roughness by different methods, empirical methods statistical methods, fractal dimension methods and 2-digits code base on observation. Compare the different methods in order to find the best-correlated methods also, if one or more of these methods could be useful to distinguish between lab generated surfaces and natural surfaces.

Results and discussion

Fractures surfaces roughness in Luxembourg Sandstone (Ernzen quarry) has an important influence on fluid flow. Fracture roughness, which is the difference between the maximum and minimum surface asperity height (Slottke, 2010), has been analysed in the quarry using visual observation (scale 1-3) and a gauge device then compared to the ten roughness profiles (Barton & Choubey, 1977). The study shows that the majority of the fractures in Luxembourg Sandstone (Ernzen quarry) have smooth to moderately rough surfaces.

Studying the mechanical properties of Luxembourg Sandstone, type of fractures and tectonic context reveal a clear connection between the most abundant type of fractures, tension fractures and low resistance for tensile deformation (Rt=4.4 MPa) and the least abundant types of fracture (compressive and shear) and moderate to high resistance for compressive deformation (Rc=60MPa) and high resistance for shear deformation (τ between 25–87 MPa).

In addition, using high precision laser scans and different methods including statistical methods (Z2 (root mean square), Ra (average height of asperities), σ_a (standard deviation of asperities heights), fractal dimension methods (semi-variogram (Dvar), Yardstick (Dyard)) and JRC (Turk et al., 1987) to analyse natural and lab generated surfaces (tensile + shear) indicate a very good correlation between Z2 and Dyard (R^2=0.96) and between Z2 and JRC (Turk et al., 1987) (R^2=0.92).

Comparing natural surfaces roughness parameters with lab generated (tensile +shear) surfaces roughness parameters shows Z2, Dyard and JRC (Turk et al., 1987) are useful to distinguish between natural surfaces and lab generated surfaces (tensile + shear). Lab generated surfaces (tensile + shear) parameters (Z2, Dyard and JRC (Turk et al., 1987)) have lower values comparing to natural surfaces parameters. Comparing our results with a previous study in chalk (Wattier et al., 2018) indicates that analysing fractures roughness using the previous methods is sensible and promising for use in a different type of rocks.

References

Barton, N. & Choubey, V., 1977. The shear strength of rock joints in theory and practice. Rock Mechanics, 10, 1-54. https://doi.org/10.1007/BF01261801

Slottke, D.T., 2010. Surface roughness of natural rock fractures: implications for prediction of fluid flow. Unpublished Ph.D. Thesis, University of Texas, Austin, 234 p.

Turk, N., Gerd, M.J., Dearman, W.R. & Amin, F.F., 1987. Characterization of rock joint surfaces by fractal dimension. In Farmer I.W., Daemen, J.J.K., Desai, C.S., Glass, C.E. & Neuman, S.P. (eds), Rock Mechanics: Proceedings of the 28th US Symposium, Tucson, Arizona. Rotterdam, Balkema, 1223–1236.

Wattier, L.M., Descamps, F., Vandycke, S. & Tshibangu, J.-P., 2018. Chalk fractures geometry: a comprehensive description of fracture surfaces. In Lawrence, J.A., Preene, M., Lawrence, U.L. & Buckley, R., Engineering in Chalk 2018: Proceedings of the Chalk 2018 Conference, Imperial College, London. ICE Publishing, London, 663-668.

Zimmerman, R.W. & Bodvarsson, G.S., 1996. Hydraulic conductivity of rock fractures. Transport in Porous Media, 23, 1-30. https://doi.org/10.1007/BF00145263

Special thanks to Mons University (Pr Jean-Pierre Tshibangu, Pr Fanny Descamps, Ir Nicolas Gonze, Geologist Ophelie Fay, Ir Temenuga Georgieva and Technician Damien Bury). Special thanks to ULB (Pr Daniel Demaiffe, Pr Alain Bernard, Pr Nadine Mattielli, and Technician Georges Zaboukis). Special thanks to Geologist Paul Wertz in Ernzen quarry.

Hypoxia on the NW Black Sea shelf during the Holocene: insights from geochemical and mineralogical proxies

SARAH ROBINET[1*] & NATHALIE FAGEL[1]

[1] *University of Liège, Department of Geology, Liège, Belgium.*
**corresponding author: sarah.robinet@alumni.uliege.be.*

Desoxygenation of the oceans and particularly coastal hypoxia ($[O_2] < 2$ mg L^{-1}) is a growing concern. Since the 1970's, seasonal hypoxia has been documented on the north-western Black Sea shelf. Hypoxia occurs during summer and early autumn due to a reinforcement of the stratification. However, little is known about oxygenation levels in coastal areas of the Black Sea during the Holocene. The aim of this work was to detect past periods of oxygen restriction potentially recorded in the sediments. Two gravity cores were retrieved in the framework of the BenthOx project (FNRS PDR T.1009.15): the GC7 core located in front of the Danube mouth (45°12'N, 29° 48'E; 2.15 m long) and the GC15 core situated in the Odessa Bay (46°31'N, 30°47'E; 2.97 m long). Both cores are located at less than 5 km from the coast, under 20 m water depth. Several proxies for past hypoxia were tested, i.e. organic matter content, redox-sensitive elements, reactive iron speciation and framboidal pyrite diameters.

Peaks of organic carbon can be used as a proxy to highlight hypoxic periods. The organic carbon content was thus measured by an elemental analyzer. However, no significant peaks were detected. The GC15 core contains, on average, slightly more organic carbon (1.9 wt%) than the GC7 core (1.1 wt%).

Among redox-sensitive elements, vanadium (measured by ICP-MS) is highly correlated with aluminium (measured by ICP -OES) in both cores and thus behaves as a detrital element. In GC15, uranium (measured by ICP-MS) is slightly enriched (with an enrichment factor of 1.5 compared to the average upper crust abundance). The average low Mo concentration (~1 ppm) measured by LA-ICP-MS in three intervals (~1 cm long) suggests the absence of euxinic conditions (i.e. with free H_2S in the water column). In this study, the X-Ray Fluorescence core scanner (XRF scan) data seem not reliable enough to allow the detection of hypoxia due to the following reasons. (1) The hypoxic periods suggested by punctual high Fe/Ti and S/Ti values (measured by XRF scan) were not further validated by the framboidal pyrite observations. (2) The low range of elemental variations measured by ICP-MS and ICP-OES does not allow to calibrate the XRF scan data. (3) The number of counts in XRF scan depends on the element but also on many factors such as water and organic contents, grain size and surface irregularities.

Based on sequential extraction, the pyrite fraction corresponds to only 6 ± 2% of reactive iron in the whole GC7 core. In contrast, the GC15 core shows an increase in pyrite downwards (from 20% up to 80% of reactive iron) and a decrease in the Fe_{ox} (hematite and goethite) and the Fe_H (FeS, siderite, ferrihydrite, akaganeite and lepidocrocite) fractions (from 20% to 3% and from 50% to 11%, respectively). This iron reduction with depth is linked to the decomposition of organic matter within the sediment during diagenesis. However, it provides no clear indication concerning the water column oxygenation.

Finally, the last proxy was the size distribution of framboidal pyrites. In GC7, no pyrite was detected by X-Ray Diffraction (XRD) and no framboidal pyrites were observed with the scanning electron microscope (SEM). The absence of framboidal pyrites in this core would be linked to oxic bottom waters. On the contrary, in GC15, XRD detects traces of pyrite and SEM observations show framboidal pyrites. Based on the measurements of 30 diameters per sample, two groups of framboidal pyrites were identified. The first group is characterized by a mean diameter between 3 and 6 µm with a narrow standard deviation (1 or 2 µm), while the second group presents a larger mean diameter (from 6 to 10 µm) with a wider standard deviation (3 to 5 µm). The smaller framboid group is supposed to form in an anoxic water column (i.e. no oxygen at all). The bigger framboid group is assumed to grow within the sediment under dysoxic (i.e. low oxygen content, considered here as a synonym of hypoxic) or oxic bottom waters.

In conclusion, oxygenation conditions are not similar in the two coastal sites studied. Near the Danube mouth (GC7), the absence of framboidal pyrites suggests oxic conditions. On the contrary, in the Odessa Bay (GC15), the framboidal pyrite proxy records an alternation between anoxic and hypoxic/oxic bottom waters. Future research should determine the presence or absence of framboidal pyrites in suspension in the water column of the Black Sea shelf during the hypoxic summer period.

Understanding the geological history of Mars by dating Martian meteorites

JÉRÔME ROLAND[1,2*], VINCIANE DEBAILLE[1] & GENEVIÈVE HUBLET[1]

[1]*Laboratoire G-Time, Université Libre de Bruxelles, Brussels, Belgium.*
[2]*AMGC, Vrije Universiteit Brussel, Brussels, Belgium.*
** corresponding author: jeroland@ulb.ac.be.*

Mars is the most distant terrestrial planet from the Sun and the second smallest. The planet arose much of interest over the last decades with the search of extra-terrestrial life. But the study of Mars is not limited to astrobiology. Indeed, Mars might be analogous to the early Earth and the study of Martian geology can provide many information about planetary formation and differentiation mechanisms. There has not been yet a sample return mission from the surface of Mars. The only Martian material available to this present day is meteorites. The Martian meteorites are mainly represented by the shergottites, nakhlites and chassignites, also known as the SNC group. Five Martian meteorites have been studied during this project: Caleta el Cobre (CeC) 022 a newly discovered nakhlite and Asuka (A) 12325, North West Africa (NWA) 11339, NWA10961 and NWA11261, all shergottites. The samples were all crushed, dissolved in acid and measured for their major and trace elements contents. Three of these samples, CeC022, A12325 and NWA11339, were also crushed and separated according to their mineralogy. These fractions were then purified using columns chromatography and measured on ICP-MS in order to obtain ^{147}Sm-^{143}Nd and ^{176}Lu-^{176}Hf data to build their isochrons. CeC022, A12325 and NWA11339 have a Sm-Nd crystallization age of 1216 ± 67, 394 ± 61 and 169 ± 40 million years (Myr) respectively and a Lu-Hf age of 1103 ± 230, 272 ± 39 and 110 ± 34 Myr. CeC022 is one of the youngest nakhlite ever found and shares geochemical and petrographical features with both of the already established groups of nakhlites. These two groups differ essentially by their cooling rates, one showing rapid cooling rates and the other slower rates. The petrogenetic model of a single pile of cumulates cannot explain the shared characteristics of CeC022 with the two groups of nakhlites and must be abandoned. Therefore, a new model must be proposed, with a more complex magmatic system composed of multiple flows. The trace elements profiles indicate that A12325, NWA10961 and NWA11261 are depleted shergottites, meaning they are depleted in incompatible trace elements. NWA11261 shows a strong terrestrial alteration. The crystallization age of A12325 is concordant with the range of crystallization ages found in the literature, from 160 to 570 Myr, with enriched shergottites being younger and the depleted older. NWA113399 is an enriched shergottite with a young crystallisation age concordant as well with the literature. The shergottites formed a broad group of meteorites with a large compositional and mineralogical diversity difficult to interpret. $\varepsilon^{143}Nd_i$ and $\varepsilon^{176}Hf_i$ were calculated for the two dated shergottites: A12325 has epsilon values of +6.6 ± 3.1 et +29.6 ± 0.3 respectively and NWA11339 values of -7.4 ± 1.4 et -17.8 ± 0.5. The epsilons of A12325 are much lower than the ones found in the literature but the epsilons of NWA11339 are concordant. The $\varepsilon^{142}Nd$ of CeC022 has been determined and has a value of +0.56 which is slightly lower than the values found in the literature.

Acknowledgments

The authors would like to thank Akira Yamaguchi (NIPR, Tokyo) for furnishing A12325, Jérôme Gattacceca (CEREGE, Aix-en-Provence) for CeC022 as well as Ben and William Hoefnagels for the three NWA. The authors would also like to thank Sabrina Cauchies for the help in the lab and Hamed Pourkhorsandi for the measurements on the TIMS.

Improving a flow meter device for long term cave dripping monitoring

ANTOINE SCOHIER

University of Mons, Faculty of Engineering, Geology and Applied Geology, Rue de Houdain 9, 7000 Mons, Belgium.

The following document describes the development and improvement of a flow meter for long term cave dripping monitoring relying on Arduino and Raspberry Pi. The document first describes the problem and the measurement environment before synthesizing the already existing solutions in the scientific literature and the flow meter developed by the department of *Geology and Applied Geology* at *Faculty of Engineering of Mons*. The solution from *G&AG* is discussed to identify its possible flaws and propose improvements. New flow meters designs are proposed. Based on the same technique to measure flow rates, namely calculating the derivate of water volume over time, a new V2 Sensor is developed for better quality results and a more stable measurement. Then, tests in the laboratory will determine that the Arduino and Raspberry Pi are safe and reliable to work in an unfavorable environment as the perturbations induced by the two most important parameters in a cave, temperature and humidity, don't alter the measurements significantly. A first flowmeter is conceived as a Tipping-Bucket device and tested in the field. The device, whose working principle consists in an upstream bucket tipping the water into a downstream recipient while a level sensor logs the height variations, is found to be too sensitive to external perturbations and the choice of a siphon to drain the water out of the recipient multiplies the issues when working at a low flow rate. Therefore solenoid valves are introduced to replace the siphon's emptying problem and new flow meter prototypes are conceived. Multiple solutions are manufactured and tested in the laboratory. First a Single Tank Electrovalve Controlled Device is discussed but is quickly put to the side due to his high data loss and inability to integrate the total flow, resulting in the

discussion of a Double Tank Electrovalve Controlled Device. The first one developed used the tanks in parallel, which gave significant results for high flow rates but quickly overheated when the flow rate decreased under approximatively 5 L/h. Finally, the final solution is developed using the tanks in serial. This last device presents high quality measurement using V2 Sensor for low and high flow rate measurements whose relative errors do not exceed 2%. The device was then tested in *Rochefort Cave Laboratory* and was able to show the effect of a storm on infiltration rates.

Tsunamigenic potential of submarine landslides on passive margins: Case study for the Irish margin

LOTTE VERWEIRDER[1*] & DAVID VAN ROOIJ[1]

[1]*Renard Centre of Marine Geology (RCMG), Department of Geology, Ghent University, Krijgslaan 281 S8, 9000 Ghent, Belgium.*
[*]*corresponding author: Lotte.Verweirder@UGent.be.*

Most tsunamis we know of were triggered by megathrust earthquakes in active continental margins (e.g. Lay et al., 2005; Lorito et al., 2011), but tsunamis generated by submarine landslides on passive margins have more recently also been recognized (e.g. Bondevik et al., 2005; Løvholt et al., 2017; Salmanidou et al., 2017). In the Porcupine Seabight, an oceanic basin close to the southwest coast of Ireland, multiple sources report evidence of past landslide activity (Kenyon et al., 1998; Huvenne et al., 2002; Wheeler et al., 2003). Yet, the area has so far received very little attention within the context of risk assessment related to landslide-generated tsunamis.

To make a start in this risk assessment, three areas were selected on the eastern slope of the Porcupine Seabight: two where the geomorphology indicates past slope instability, and one where a break in the bathymetry could hint at slope failure in the future. All three areas are situated on the flanks of submarine channels that are part of the Kings Channel System or Gollum Channel System.

Bathymetry and 2D reflection seismic data are used to determine various landslide characteristics that have an influence on the wave that the landslide generates (thickness, volume, landslide dynamics, water depth, setting within the channels…; Harbitz et al., 2006). Furthermore, these two datasets are also used to analyse the possible processes and/or events that are involved in triggering the landslides, the most probable failure mechanisms, and the timing of the slope failures. A final step in the risk assessment is to judge how the landslide properties affect the generated tsunamis. This is only done in a qualitative manner, through literature study and comparison with other landslides.

From this investigation, it seems that the build-up of an excess in pore pressure within the sediments, possibly linked to elevated sedimentation rates during the deglaciation of the British-Irish Ice Sheet (BIIS) after the Last Glacial Maximum, is the main process weakening the slope sediments in all three areas. It is generally thought that a final trigger is needed to actually make the (weakened) slope fail and cause a landslide (Vanneste et al., 2014), and for the study area this could be an earthquake generated from glacio-isostatic rebound related to the deglaciation of the BIIS. Taking these factors into account, an approximate date of 20,000 cal yrs BP is suggested as a time of slope instability in the study area. From the assessment concerning the tsunami generation from the three landslides, it appears that the volumes of the landslides are too small and the study area too far away from the Irish shore to (have) create(d) any significant run-up.

As this is the first risk assessment related to landslide-generated tsunamis that is made for the eastern slope of the Porcupine Seabight, there is still room for improvement. Further research should include expanding the 2D reflection seismic dataset in several parts of the study area, coring to test the hypothesis concerning the timing of the events, and geotechnical tests to provide more accurate values for some of the landslide properties, so that they can be used in modelling. Thus, the effects on the tsunami wave generation can be quantified, which would make the risk assessment much more accurate.

References

Bondevik, S., Løvholt, F., Harbitz, C.B., Mangerud, J., Dawson, A. & Svendsen, J.I., 2005. The Storegga Slide tsunami - comparing field observations with numerical simulations. Marine and Petroleum Geology, 22, 195–208. https://doi.org/10.1016/B978-0-08-044694-3.50021-4

Harbitz, C.B., Løvholt, F., Pedersen, G. & Masson, D.G., 2006. Mechanisms of tsunami generation by submarine landslides: A short review. Norwegian Journal of Geology, 86, 255–264.

Huvenne, V.A.I., Croker, P.F. & Henriet, J.-P., 2002. A refreshing 3D view of an ancient sediment collapse and slope failure. Terra Nova, 14, 33–40. https://doi.org/10.1046/j.1365-3121.2002.00386.x

Kenyon, N.H., Ivanov, M.K. & Akhmetzhanov, A.M., 1998. Cold water carbonate mounds and sediment transport on the Northeast Atlantic margin. IOC Technical Series, 52, 178 p.

Lay, T., Kanamori, H., Ammon, C.J., Nettles, M., Ward, S.N., Aster, R.C., Beck, S.L., Bilek, S.L., Brudzinski, M.R., Butler, R., DeShon, H.R., Ekström, G., Satake, K. & Sipkin, S., 2005. The Great Sumatra-Andaman Earthquake of 26 December 2004. Science, 308, 1127–1133. https://doi.org/10.1126/science.1112250

Lorito, S., Romano, F., Atzori, S., Tong, X., Avallone, A., McCloskey, J., Cocco, M., Boschi, E. & Piatanesi, A., 2011. Limited overlap between the seismic gap and coseismic slip of the great 2010 Chile earthquake. Nature Geoscience, 4, 173–177. https://doi.org/10.1038/ngeo1073

Løvholt, F., Bondevik, S., Laberg, J.S., Kim, J. & Boylan, N., 2017. Some giant submarine landslides do not produce large tsunamis. Geophysical Research Letters, 44, 8463–8472. https://doi.org/10.1002/2017GL074062

Salmanidou, D.M., Guillas, S., Georgiopoulou, A. & Dias, F., 2017. Statistical emulation of landslide-induced tsunamis at the Rockall Bank, NE Atlantic. Proceedings of the Royal Society A: Mathematical, Physical and Engineering Sciences, 473, 20170026. https://doi.org/10.1098/rspa.2017.0026

Vanneste, M., Sultan, N., Garziglia, S., Forsberg, C.F. & L'Heureux, J.-S., 2014. Seafloor instabilities and sediment deformation processes: The need for integrated, multi-disciplinary investigations. Marine Geology, 352, 183–214. https://doi.org/10.1016/j.margeo.2014.01.005

Wheeler, A.J., Kenyon, N.H., Ivanov, M.K., Beyer, A., Cronin, B.T., McDonnell, A., Schenke, H.W., Akhmetzhanov, A.M., Satur, N. & Zaragosi, S., 2003. Canyon heads and channel architecture of the Gollum Channel, Porcupine Seabight. In Mienert, J. & Weaver, P. (eds), European Margin Sediment Dynamics: Side-Scan Sonar and Seismic Images. Springer, Berlin, 183–186. https://doi.org/10.1007/978-3-642-55846-7_29

Available online 27.08.2020.